VOL. 10, NO. 21, NOVEMBER 2015 ISSN 1819-6608
ARPN Journal of Engineering and Applied Sciences
©2006-2015 Asian Research Publishing Network (ARPN). All rights reserved.

www.arpnjournals.com

LOW TEMPERATURE SOLDER ALLOYS FOR ULTRASONIC SOLDERING OF GLASS

Mustafa M.Y., Hilmy I. and Adesta E. Y. T.
School of Materials and Manufacturing Engineering, Faculty of Engineering, International Islamic University Malaysia
E-Mail: my@royalselangor.com.my

ABSTRACT

The research focused on improving the adhesion of low melting temperature lead free solders to soda lime glass through ultrasonic soldering. All soldering parameters involving temperature, time, vibration amplitude and frequency were kept constant except for the new alloying elements to Sn40Bi solders. Improvement on adhesion strength of Sn40Bi solders was attempted by alloying with Al, Mg, Zn and Ag elements. Tensile test was applied on soldered specimen to determine shear separation strength. The positive effect of metal oxide passivation from alloying elements was observed on the adhesion strength. Tensile test and thermogravimetry analysis were applied to determine mechanical and chemical properties of selected solder alloys (Sn40Bi) 0.3 Mg and (Sn40Bi) 0.5Al. Scanning electron microscope (SEM) and energy dispersive X-ray spectroscopy (EDX) were used to examine the bonding mechanism of the selected solders to glass. Sn and Bi were observed to remain in metallic form without adhering to glass. Mg and Al were observed to passivate to metal oxide form. MgO from (Sn40Bi) 0.3 Mg forms metal oxide bond to glass. Al_2O_3 from (Sn40Bi) 0.5Al forms metal oxide bond to glass.

Keywords: ultrasonic soldering; metal oxide bond; glass soldering; bonding mechanism; PB-free solder.

INTRODUCTION

Ultrasonic soldering (US) technique is able to bond difficult to solder substrates together. Bonding is achieved by combining heat and ultrasonic vibration through suitable solder alloy. The research focused on the development of low melting temperature lead free solder alloys to solder soda lime glass and pewter (Sn5Sb1.2Cu by wt%) with solidus temperature of 222.4 °C. Giftware products combining glass and Sn5Sb1.2Cu require good match up for strong adhesive bonding. Adhesive bonding is weakened by gaps in between. Bonding by US requires only moderate matching up by having molten solder filling up the gaps. US adhesion strength is affected by soldering time [1, 2] and soldering temperature [3, 4]. Variations in both parameters affect the liquid fraction, diffusion and intermetallic compound formation of solder alloys. Higher vibrational amplitude assists in the spreading of solder alloys [5]. Ultrasonic frequency ranges from 19 to 60 kHz with higher frequency for difficult to solder parts [3 - 11].

US for Al alloys mainly uses various compositions of Zn, Al and Sn as solder alloys. Zn-Al and pure Sn filler metals were used to determine optimum soldering time for US joining of 2024 Al [1, 2]. Diffusion of Al and alumina substrates into the filler metals strengthens the joint. US of 5056 Al joints was conducted using Zn-Al and Zn-Sn solder alloys [3, 4]. US was conducted on 1070 Al using Sn23Zn solder alloy [1]. In non US setting, addition of 0.3 wt. % Ag to Sn-9Zn-xAg improves the solder alloy microstructures, wettabilities and mechanical properties due to increasing oxidation resistance [12]. Zn-Al-Mg-Ga solder produces higher die shear strength and may replace leaded Pb5Sn solder for Si die attachment with Cu lead-frame in automatic die attach machine [13].

Development of low temperature solder alloys was conducted by selecting Sn40Bi by wt% as the base solder alloy. Sn40Bi has solidus temperature of 138 °C and liquids temperature of 170 °C [14]. The low melting temperature is ideal for soldering glass and Sn5Sb1.2Cu without damaging the surface of substrates. By itself, Sn40Bi solder alloy failed to adhere to glass using US. Al, Mg, Zn and Ag were selected as alloying elements to improve Sn40Bi adhesion property to glass. The shear separation strength of soldered specimen between glass and Sn5Sb1.2Cu was measured by tensile test.

MATERIALS AND METHODS

US was conducted using a device, Sunbonder USM-5 from Kuroda Techno with adjustable soldering temperature ranging from 200 – 500 °C and vibration power at 1 -12 Watt with fixed frequency at 60 kHz. Sn40Bi as the base solder alloy was prepared by adding Bi (40 wt%) into molten Sn in an electric pot set at 500 °C. Small granules of Al, Mg, Zn and Ag as alloying elements were weighed, added and stirred separately to molten Sn40Bi. Smooth flow of solder alloys is important for uninterrupted soldering. Mg proportion was limited to 0.5% (wt%) due to its high viscosity at molten stage. Ag was limited to 1.25% (wt%) due to high cost involved. Al and Zn were limited to 5% (wt%) with solder flow remaining smooth. The compositions of the selected 24 solder alloys with added Al, Mg, Zn and Ag are shown in Table-1.

The solder alloys were cast into 2mm diameter rod and cut to granule at uniform weight of 0.10 gram. Soda-lime-silica glass was used as substrate. 2 mm thick glass panel was cut to dimensions of 33 x 16 mm. Sn5Sb1.2Cu substrate was alloyed by adding small granules of Sb (5 wt%) and Cu (1.2 wt %) into molten Sn in an electric pot and cast in a steel mold. The cast sheet was rolled to thickness of 2 mm and guillotined into dimensions of 55 x 20 mm.

©2006-2015 Asian Research Publishing Network (ARPN). All rights reserved.

Table-1. Compositions of Sn40Bi solders alloyed with Al, Mg, Zn and Ag.

Solder Alloys	'x; by weight %					
(Sn40Bi)xAl	0.5	1.0	2.0	3.0	4.0	5.0
(Sn40Bi)xMg	0.1	0.2	0.3	0.4	0.5	0.6
(Sn40Bi)xZn	0.5	1.0	2.0	3.0	4.0	5.0
(Sn40Bi)xAg	0.05	0.25	0.5	0.75	1.00	1.25

A soldering apparatus shown in Figure-1 was fabricated for holding of glass and Sn5Sb1.2Cu plates in lap joint position. It was fitted with 150 W electrical heater set at optimum temperature of 150 °C. The temperature was ideal, as lower setting inhibited solder flow while higher setting delayed solders solidification. The heater was added to ensure fast soldering cycle. The apparatus heater was switched on. Glass plate was wiped clean with petrol and cloth and inserted into the apparatus. The oxide layer on the sides of Sn5Sb1.2Cu plate was scrapped by knife and inserted into the apparatus. The solder granule was placed on glass surface when surface temperature reached 150 °C. US tool tip was set at 450 °C and vibration amplitude at 8W. Solder granule melted upon contact to the tool tip. The plates bonded when vibrating tool tip was rubbed throughout the glass surface and the edge of Sn5Sb1.2Cu for 30 seconds. The same process was repeated on the opposite segment. US for each solder alloy was replicated on 4 glass and pewter specimens. Heater was switched off and soldered specimen removed upon cooling to room temperature. The combined soldered area on glass is at 1.12 cm^2 while the soldered area for Sn5Sb1.2Cu is at 0.64 cm^2.

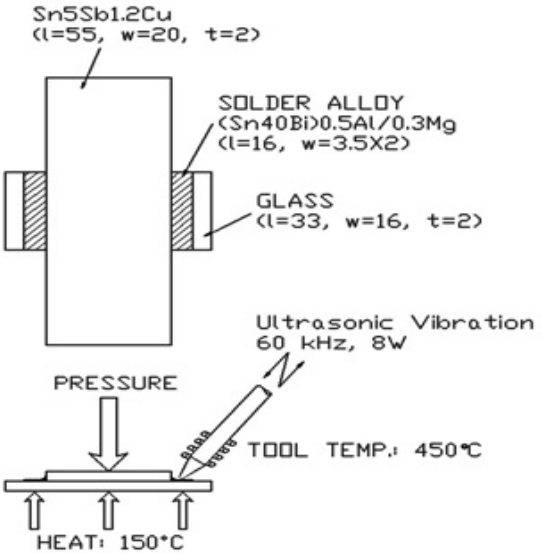

Figure-1. Schematic diagram of soldering apparatus.

An apparatus shown in Figure-2 was fabricated for holding the soldered specimen during tensile test. The apparatus with soldered specimen was clamped in Instron 5582 tension testing machine. Tensile test rate was set at 2 mm/ min at room temperature. Shear separation strength measurements were based on the average of 4 replications.

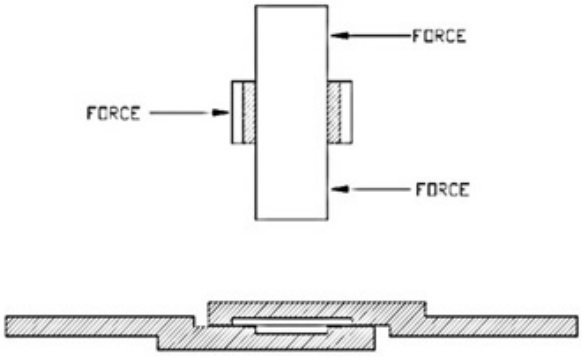

Figure-2. Schematic diagram of tensile test apparatus.

Evaluation of shear separation strength values resulted in selection of (Sn40Bi) 0.3Mg and (Sn40Bi) 0.5Al. Experimentations were conducted on the properties of the two selected solder alloys. The chemical compositions of both solder alloys are listed in Table 2. In addition, the mechanical properties of both solder alloys were evaluated and obtained using Instron 5582 tension testing machine.

Table-2. Chemical compositions of (Sn40Bi) 0.5Al and (Sn40Bi) 0.3Mg.

Material	Sn	Bi	Al	Mg	Others
(Sn40Bi)0.5Al	59.64	39.76	0.50	-	Bal.
(Sn40Bi)0.3Mg	59.76	39.86	-	0.30	Bal.

The solidus and liquidus temperatures for both solder alloys were obtained using Hitachi STA7300 thermogravimetric analyzer. Characterization was conducted only on solder joint between glass specimens soldered with (Sn40Bi) 0.5Al and (Sn40Bi) 0.3Mg solders. This is due to fracture not detected between solders and Sn5Sb1.2Cu during tensile test. SEM micrographs were taken using JEOL JSM-6700F for both solder joints at 25000X magnification. EDX analysis using JEOL JSM-5600 at 15.0 KV on the elements and compound by wt% was conducted starting from the interface and expanding on both sides of glass and solders. The elements involved were Sn, Bi, Al, Mg, Si, Ca and Na. Subsequent measurements after the interface were taken at the intervals of 10 µm. Measurements were continuously taken until the readings of elements by wt% reached stable values.

RESULTS AND DISCUSSION

The tensile test conducted on the soldered specimen produced shear separation force and extension before fracture graph. Graph for a sample specimen is shown in Figure-3. Shear separation force is the force required to separate the soldered specimen of glass and

©2006-2015 Asian Research Publishing Network (ARPN). All rights reserved.

Sn5Sb1.2Cu. Shear separation force can be converted to shear separation strength by dividing with soldered surface area at 1.12 cm^2. Fracture only occurred between glass and solders and not between Sn5Sb1.2Cu and solders. Bond is weaker between solders and glass despite smaller soldered surface area between solders and Sn5Sb1.2Cu at 0.64 cm^2.

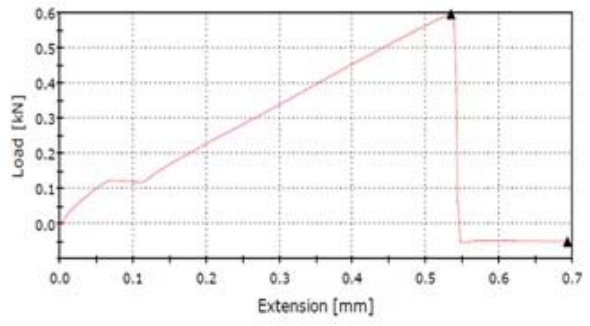

Figure-3. A sample graph of shear separation force and extension before fracture.

Shear separation strength data involving (Sn40Bi) xAl, (Sn40Bi) xMg, (Sn40Bi) xAg and (Sn40Bi) xZn solder alloys is shown in Figure-4. Sn40Bi solder alloyed with Mg and Al have higher shear separation strength. Shear separation strength peaked at 2.95 MPa for (Sn40Bi) 0.3Mg and at 2.10 MPa for (Sn40Bi)0.5Al.

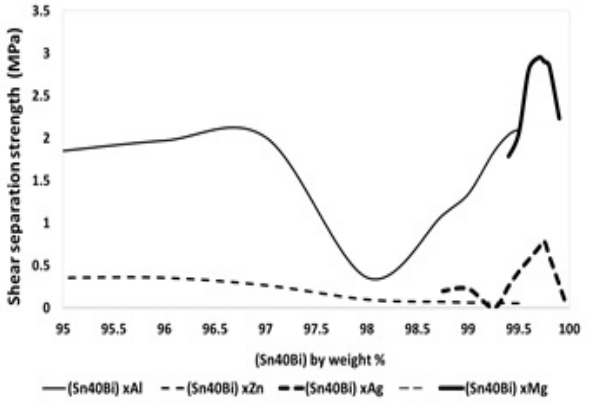

Figure-4. Graph of shear separation strength for four groups of solder alloys.

Sn40Bi did not adhere to glass during test conducted by the author. Adhesion to glass occurred due to the presence of the alloying elements Al, Mg, Ag and Zn. The alloying elements form different passivation layers when exposed to atmosphere. Al reacts with atmospheric oxygen and forms passivation layer of Al_2O_3 or aluminum oxide [15]. Mg in air forms instantaneous passivation layer of MgO or magnesium oxide at 25nm thick [16, 17]. Zn exposed for four days to air at 35 °C and 85 % RH formed oxide layer of ZnO topped with thin layer of Zn $(OH)_2$ [17]. The zinc hydroxide layer was formed from moisture in high humidity level. With continuous exposure to CO_2, ZnO forms $ZnCaO_3$. Ag is stable in pure air. In the presence of sulfide, it tarnishes to form Ag_2S [18]. Adhesion of solders to glass is stronger for alloying elements with passivated layer of metal oxide. Adsorption of oxygen by solder alloy strengthens adhesion with glass surface. Bonding between glass and solders is more conducive with the presence of metal oxide.

The derived mechanical properties of solder alloys (Sn40Bi) 0.5Al and (Sn40Bi) 0.3Mg are shown in Table 3. (Sn40Bi) 0.3Mg has both higher tensile strength and greater ductility than (Sn40Bi) 0.5Al. The mechanical properties signify that (Sn40Bi) 0.3Mg is a stronger solder metal alloy than (Sn40Bi) 0.5Al as low temperature lead free solder alloy for bonding to glass. At specific equal conditions, the solder alloy (Sn40Bi) 0.3Mg will require stronger shear separation strength to rupture in comparison to (Sn40Bi) 0.5Al.

Table-3. Mechanical properties of glass, Sn5Sb1.2Cu, (Sn40Bi) 0.5Al and (Sn40Bi) 0.3Mg.

Material	Tensile strength	Elongation
Sn5Sb1.2Cu	39.6 MPa	8.78 %
(Sn40Bi)0.5Al	70.6 MPa	5.40 %
(Sn40Bi00.3Mg	77.15 MPa	6.18 %

The phase diagram for (Sn40Bi) 0.3Mg is shown in Figure-5. The solidus temperature is at 141.6 °C while the liquidus temperature is at 170.8 °C. The phase diagram for (Sn40Bi) 0.5Al is shown in Figure-6 with solidus temperature at 143.3 °C and liquidus temperature at 171.1 °C. The difference between the solders' liquidus temperature against Sn5Sb1.2Cu solidus temperature of 222.4 °C exceeds 50 °C. Soldering can be done without damaging the surface of Sn5Sb1.2Cu and soda lime glass.

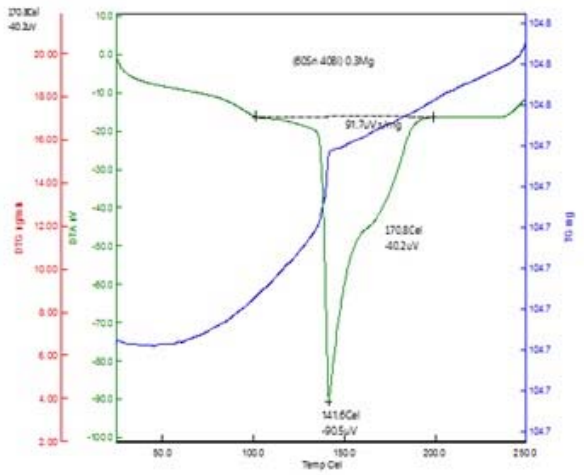

Figure-5. Phase diagram of solder alloy (Sn40Bi) 0.3Mg.

©2006-2015 Asian Research Publishing Network (ARPN). All rights reserved.

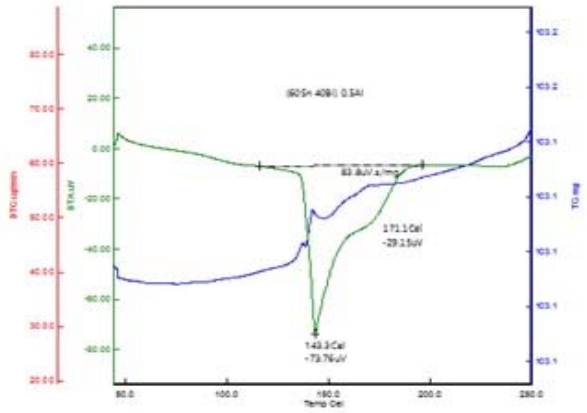

Figure-6. Phase diagram of solder alloy (Sn40Bi) 0.5Al.

The SEM micrographs at 10000 magnifications on the cross section of joint between glass and both solder alloys, (Sn40Bi)0.5Al and (Sn40Bi)0.3Mg are shown in Figure-7. Formation of intermetallic compound (IMC) is not visible at the interface between glass and both solder alloys. The absence of IMC layer signifies that the bonding mechanism is not based on diffusion of solders and migration of substrates crossing the interface. Bonding between glass and (Sn40Bi) 0.3Mg is more comprehensive without numerous gaps signifying a more complete bonding. Bonding between glass and (Sn40Bi) 0.5Al is not comprehensive with visible gaps signifying incomplete bonding. The difference is reflected by the higher shear separation strength values for (Sn40Bi) 0.3Mg when compared to (Sn40Bi) 0.5Al. In the case of ceramic and solder, their bond is in the form of metal oxide adhesion [19]. The bond between glass and solders is also in the form of metal oxide adhesion. In addition, the metal oxide adhesion bond is strengthened by formation of mechanical adhesion when molten solder flowed into the crevices of glass surface created by the strong vibration amplitude of soldering tool. The protrusions formed by flowing molten solders are visible on both (Sn40Bi) 0.3Mg and (Sn40Bi)0.5Al solder alloys.

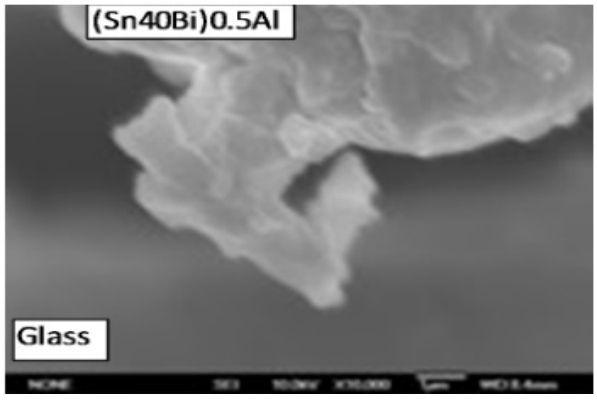

Figure-7. SEM micrographs of joint between (Sn40Bi) 0.5Al solders and glass.

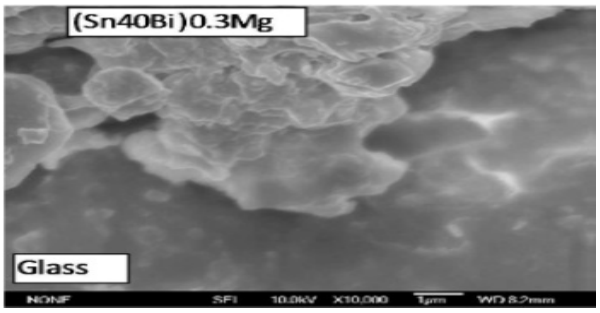

Figure-8. SEM micrographs of joint between (Sn40Bi) 0.3Mg solders and glass.

Measurements of the wt% of elements were taken through EDX analysis conducted on the cross section of solder joint between glass and the solders. Apart from the interface, 4 measurements at intervals of 10 μm were taken on both solders and glass sides. The compositions of elements and compounds by wt% reached stable values by the distance of 40 μm from the interface. The elements and compounds detected were Sn, Bi, Al_2O_3 (alumina), MgO (magnesia), Na_2O (sodium oxide), SiO_2 (silica) and CaO (lime).

The elements and compounds by wt% documented at interface between (Sn40Bi) 0.3Mg and glass are shown in Figure-9. From the solders side, Sn, Bi and MgO (magnesia) were detected. Both Sn and Bi remained in pure metallic form. Earlier test confirmed Sn40Bi did not adhere to glass. Flow of molten Sn stopped at the interface while molten Bi diffused deep into the glass region. Mg from the solder passivated completely into MgO. MgO migrated to the region within 10 μm of both sides of the interface, becoming the agent bonding solders to glass. From the glass side, Al_2O_3 (alumina), MgO (magnesia), Na_2O (sodium oxide), SiO_2 (silica) and CaO (lime) were detected. Both Al_2O_3 and MgO were part of minor additives of glass and did not migrate beyond the interface to solders region. CaO also did not migrate beyond the interface. Both SiO_2 and Na_2O migrated to beyond 40 μm into the solders region. However, SiO_2 is the likeliest agent bonding glass to MgO due to its position as the main constituent of glass. The role of Na_2O is to reduce the transition temperature of glass.

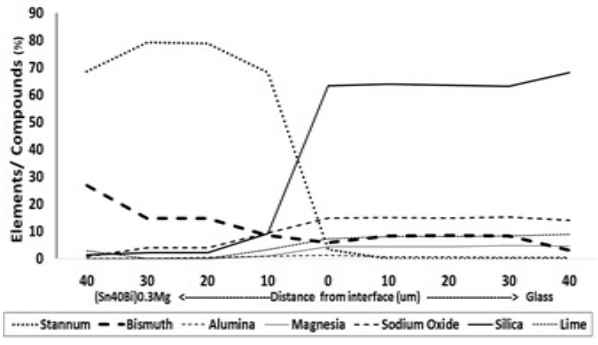

Figure-9. Elements and compounds at intermediate region between glass and (Sn40Bi) 0.3Mg solders.

©2006-2015 Asian Research Publishing Network (ARPN). All rights reserved.

The elements and compounds by wt% documented at interface between (Sn40Bi) 0.5Al and glass are shown in Figure-10. From the solders side, Sn, Bi and Al_2O_3 were detected. Both Sn and Bi remained in pure metallic form and did not adhere to glass. Flow of molten Sn stopped at 20 µm beyond the interface while molten Bi diffused deep into the glass region. Al from the solder passivated completely into Al_2O_3. Al_2O_3 migrated to the surface at the interface and 30 µm into glass region becoming the agent bonding solders to glass. On the glass side, Al_2O_3, MgO, Na_2O, SiO_2 and CaO were detected. Both Al_2O_3 and MgO were part of minor additives of glass and did not migrate beyond the interface to solders region. CaO also did not migrate beyond the interface. SiO_2 and Na_2O migrated into the solders region. SiO_2 is the likeliest agent bonding glass to Al_2O_3 due to its position as the main constituent of glass.

Research by [20] concluded that chemical bond is responsible for bonding glass plate and SnZn solders and most likely in the form of 'Zn-O-Si'. The EDX analysis based on wt% of both elements and compounds strongly suggests that SiO_2 migrated beyond 40 µm into the solders region forming metal oxide bond. The most likely metal oxide bond between (Sn40Bi) 0.3Mg and glass is 'Mg-O-Si'. The metal oxide bond between (Sn40Bi) 0.5Al and glass is 'Al-O-Si'. 'Mg-O-Si' metal oxide adhesion is stronger than 'Al-O-Si' based on shear separation strength experimental results. The bond between Mg-O-Si is likely in the form of imperfect union between Oxygen from both solder and substrate created by heat, intense pressure and ultrasonic vibration during soldering. Bond dissociation energies for Mg-O is 358.2 kJ/mol, Al-O is 501.9 kJ/mol and Si-O is 799.6 kJ/mol as shown in Table-4. The weaker ionic bond within Mg-O against Al-O resulted in stronger imperfect bond of O-O from Mg-O-Si. Stronger pull factor of Al-O resulted in weaker O-O bond within Al-O-Mg.

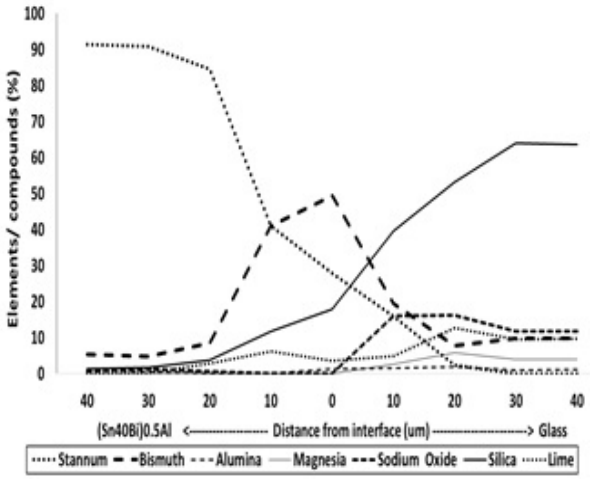

Figure-10. Elements and compounds at intermediate region between glass and (Sn40Bi) 0.5Al solders.

Table-4. Bond dissociation energies in diatomic molecules [21].

Materials	Bond dissociation energies (kJ/mol)
Al-O	501.9±10.6
Mg-O	358.2±7.2
Si-O	799.6±13.4

CONCLUSIONS

Study on low temperature solder alloys for ultrasonic soldering of glass reached the following conclusions. The adhesions of solders to glass are stronger for Sn40Bi solders alloyed with Mg or Al than Ag or Zn. This is due to both Mg and Al forming passivated layer of metal oxide. SEM observations of cross section of solder joints between glass and solder alloys (Sn40Bi) 0.3Mg and (Sn40Bi) 0.5Al did not show any IMC layer at the interface. The metal oxide adhesion between glass and solders is most likely in the form of Mg-O-Si for (Sn40Bi) 0.3Mg and Al-O-Si for (Sn40Bi) 0.5Al. (Sn40Bi) 0.3Mg formed stronger bond with smooth glass surface than (Sn40Bi) 0.5Al. The stronger bond is likely due to weaker ionic bond within MgO as compared to Al_2O_3 resulting in stronger metal oxide bond with SiO_2. Bonding between glass and solder alloys (Sn40Bi) 0.3Mg and (Sn40Bi) 0.5Al is a combination of metal oxide adhesion and mechanical adhesion.

ACKNOWLEDGEMENTS

The authors are grateful to Agile and Sustainable Manufacturing Research Unit (ASMARU) of International Islamic University of Malaysia and Royal Selangor International for the support given in this research.

REFERENCES

[1] Xu, Z., Ma, L., Yan, J., Yang, S. & Du, S. 2000. Wetting and oxidation during ultrasonic soldering of an alumina reinforced aluminum–copper–magnesium (2024 Al) matrix composite. Composites: Part A 43, 407–414.

[2] Li, Y.X., Leng, X.S., Cheng, S. & Yan, J.C. 2012. Microstructure design and dissolution behavior between 2024 Al/Sn with the ultrasonic-associated soldering. Materials and Design 40. 427–432.

[3] Nagaoka, T., Morisada, Y., Fukusumi, M. & Takemoto, T. 2011. Selection of soldering temperature for ultrasonic-assisted soldering of 5056 aluminum alloy using Zn–Al system solders. Journal of Materials Processing Technology 211(9) 1534–1539.

[4] Nagaoka, T., Morisada, Y., Fukusumi, M. &Takemoto. T. 2010. Ultrasonic-Assisted Soldering of 5056 Aluminum Alloy Using Quasi-Melting Zn-Sn Alloy. Metallurgical and Materials Transactions B: Process Metallurgy and Materials Processing Science

©2006-2015 Asian Research Publishing Network (ARPN). All rights reserved.


41 (4), 864-871.

[5] Nagaoka, T., Morisada, Y., Fukusumi, M. & Takemoto. T. 2009. Joint strength of aluminum ultrasonic soldered under liquidus temperature of Sn–Zn hypereutectic solder. Journal of Materials Processing Technology 209 5054–5059.

[6] Li, Y.X., Zhao, W.W., Leng, X.S., Fu, Q.J., Wang, L. & Yan, J.C. 2011. Microstructure evolution and mechanical properties of ultrasonic-assisted soldering joints of 2024 aluminium alloys. Trans. Non ferrous Met. Soc. China. 2. 1937 –1943.

[7] Ding, M., Zhang P.L., Zhang, Z.Y. & Yao S. 2010. A novel assembly technology of aluminum alloy honeycomb structure Int J Adv Manuf Technol 46:1253–1258.

[8] Kim, W.C., Lee, K.W., Saarinen, I.J., Pykari, L. & Paik, K.W. 2012. Ultrasonic Bonding of Anisotropic Conductive Films Containing Ultrafine Solder Balls for High-Power and High-Reliability Flex-On-Board Assembly IEEE Transaction on Components, Packaging and Manufacturing Technology, Vol. 2, No. 5.

[9] Lee, K.W., Saarinen, I.J., Pykari, L. & Kyung, W.P. 2011. High Power and High Reliability Flex-On-Board Assembly Using Solder Anisotropic Conductive Films Combined with Ultrasonic Bonding Technique. IEEE Transaction on Components, Packaging and Manufacturing Technology, Vol. 1, No. 12.

[10] Tamuraa, S., Tsunekawa, Y., Okumiya, M. & Hatakeyama, M. 2008. Ultrasonic cavitation treatment for soldering on Zr-based bulk metallic glass. Journal of Materials Processing Technology. 206 322–327.

[11] Yamada, M., Nobuhiko, C. & Takayuki. M. 2009. Solder Alloy For Bonding Oxide Material, And Solder Joint Using The Same. (Patent application number: 20090104071).

[12] Chen, W.X., Xue, S.B., & Wang. H. 2010. Wetting properties and interfacial microstructures of Sn-Zn-xGa solders on Cu substrate. Materials and Design 31. 2196-2200.

[13] Haque, A., Lim, B. H., Haseeb, A., S., M., A., Masjuki, H., H. 2012. Die attach properties of Zn–Al–Mg–Ga based high-temperature lead-free solder on Cu lead-frame. J Mater Sci: Mater Electron 23:115–123.

[14] Mei, Z. Q., Holder, H. A., & Vander Plas, H. A. (1996). Low-Temperature Solders August 1996 Hewlett-Packard Journal Article 10.

[15] Ekuma, C.E., Idenyi, N.E., & Umahi, A.E. 2007. The effects of zinc additions on the corrosion susceptibility of aluminum alloys in various tetraoxosulphate (VI) acid environments. Journal of Applied Sciences (2): 237-241.

[16] Ono, S. 1998. Surface phenomena and protective filmgrowth on magnesium and magnesium alloys Metallurgical Science and Technology Vol 16, No.2.

[17] Diler, E., Lescop, B., Rioual, S., Nguyen Vien, G., Thierry, D., Rouvellou, B. 2014. Initial formation of corrosion products on pure zinc and $MgZn_2$ examinated by XPS. Corrosion Science 79. 83-88.

[18] Mueller, H. J. 2000. In vitro tarnish and corrosion of a consolidated silver material for direct filling applications. Dental Materials 17, 60 – 70.

[19] Finnis, M.W. 1996. The theory of metal–ceramic interfaces J. Phys.: Condens. Matter **8**: 5811–5836.

[20] Yonekura, D., Ueki, T., Tokiyasu, K., Kira, S., Wakabayashi, T. 2014. Bonding mechanism of lead-free solder and glass plate by ultrasonic assisted soldering method. Materials and Design 65 907-913.

[21] Lou, Y. R., 2010. Bond dissociation energies http://staff.ustc.edu.cn/~luo 971/2010-91-CRC-BDEs-Tables.pdf (accessed 17 September 2015).